中國機械工程學刊第四十二卷第二期第 163~172 頁(民國一百一十年)
Journal of the Chinese Society of Mechanical Engineers, Vol.42, No.2, pp 163~172 (2021)

Research on APSO-WNN and its Application in Vibration Fault Diagnosis of Hydroelectric Generating Units

Yan-Chun Xu*, Hai-Ting Xia *, Shao-Chen Fang *and Mi Lu**

Keywords：adaptive particle swarm optimization, wavelet neural network, hydroelectric generating units, fault diagnosis.

ABSTRACT

Based on the research of wavelet neural network (WNN), an adaptive particle swarm optimization (APSO) is proposed to solve the complex nonlinear relationship between the vibration characteristics and fault types of hydropower systems. This algorithm combines characteristics of evolutionary compute and swarm intelligences. It can change inertia weight according to the states of the particle adaptively. APSO rises the training speed of wavelet neural network, and improves network training accuracy. Experiments indicate that wavelet neural network based on APSO contains a higher precision and faster speed of diagnosis, compared with back propagation (BP) neural network and wavelet neural network. The algorithm is a new method for fault diagnosis of hydroelectric generating units (HGU), and it can be effectively applied to practical engineering.

INTRODUCTION

HGU is a large combined equipment. There is a high demand in performance of electric power production department, especially in continuous work. A failure may cause chain reactions of HGU, which affects the entire device. And even the entire production process could not run properly. The importance of state monitoring and fault diagnosing forces people to do a lot of researches in the field of HGU.

Paper Received March, 2018. Revised Sepfember, 2020. Accepted October, 2020. Author for Correspondence: Hai-Ting Xia.

* *Associate Professor or Gradnate Student, Hubei Provincial Key Laboratory for Operation and Control of Cascaded Hydropower Station, China Three Gorges University, Yichang, China 443001.*

** *Associate Professor, Department of Electrical & Computer Engineering, Texas A&M University, College Station, USA 91207.*

Eighty percent of the hydro generator unit faults is related to vibration according to the literatures (Jianwei, 2016). HGU is a highly nonlinear system. The fault type and its vibration characteristics show a complex nonlinear relationship. Due to the influence of mechanical, electrical and hydraulic factors, there is a certain relationship between the vibration characteristics of HGU and the complexity and nonlinearity of fault set. Therefore, it is unable to get the matching relationship through theoretical research. Intelligent algorithm is commonly used to diagnose the fault of HGU. Artificial neural network is a network system which is constructed according to the principle and structure of biological neural networks (Mahdi, 2019- Xiaochuan, 2018). It becomes a common tool to diagnosis fault of HGU due to its powerful ability in processing parallel and nonlinear questions. The BP neural network is used more widely (Ma, 2017). However, the convergence speed of the algorithm is slow, and it is possible for the solution to fall into local minimum.

So, optimizing and improving the algorithm on the precedent basis becomes a new researching approach. For example, on the basis of BP neural network, the choquet fuzzy integration (Zhang, 2013) and APSO algorithm to BP neural network (Jiatang, 2015), which have been successfully used in the vibration fault diagnosis of HGU, are introduced. WNN is widely used in fault diagnosing due to its good pattern recognition and approximation ability. It obtains good results in the researches of locomotive roller bearings and gears (Fard, 2014) (Lifeng, 2017). Particle swarm optimization (PSO) algorithm is a kind of intelligent optimization algorithm based on cluster phenomenon. It has been successfully applied in the fault diagnosis of transformers and in the fault feature extraction of generator axes (Yanchun, 2018) (Zhenhua, 2019).

On the basis of the formula of the iteration, the particle is divided into two parts according to the different fitness. Each part of the weights matches different methods in order to achieve the purpose of adaptive optimization. Then APSO is used to search the parameters of WNN, which make the network contain high training speed and high accuracy. This algorithm can be effectively used in the vibration fault diagnosis of HGU.

WAVELET NEURAL NETWORK

Wavelet neural network is a neural network model based on wavelet analysis (Amezquita, 2016)(Cha, 2015). In the signal recognition, feature space of wavelet can be used as a signal classification. The core idea of wavelet neural network is to replace the sigmoid function in traditional BP neural networks by using the wavelet function. And wavelet transform is introduced into the neural network model. Through doing this, the learning ability of neural networks and the local property of wavelet algorithms are both considered.

$$C_{\psi} = \int_{-\infty}^{+\infty} \left|\hat{\psi}(\lambda)\right|^2 \Big/ |\lambda| d\lambda < \infty \tag{1}$$

$$\psi_{a,b}(x) = \frac{1}{\sqrt{a}} \psi\left(\frac{x-b}{a}\right) \tag{2}$$

Where $\hat{\psi}(\lambda)$ is the Fourier transform of $\psi(x)$, and wavelet function $\psi_{a,b}(x)$ can be transformed to $\psi(x)$ by stretching and translating. The parameters *a* is scale factor and *b* is displacement factor.

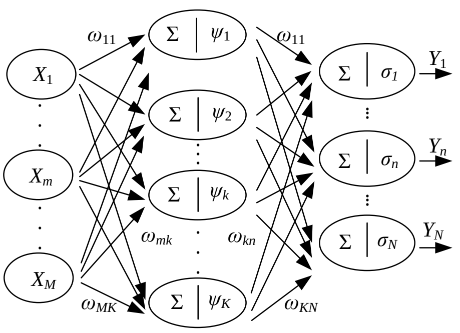

Fig. 1. The structure of a three-layer wavelet neural network.

As is shown in Figure 1, *M* is the number of input layer. The number of wavelet elements in the hidden layer is *K*. The number of output layer is *N*. The weight between the *m*-th input layer and the *k*-th hidden layer is ω_{mk}. The weight between *k*-th hidden layer and the *n*-th output layer is ω_{kn}. Wavelet basis function serves as excitation function in hidden layer. ψ_k is Morlet mother wavelet.

This wavelet is the cosine-modulated of Gauss Wavelet whose time domain and frequency domain resolution are very high. Its equation is given in (3):

$$\psi(x) = \cos(1.75x)\mathrm{e}^{-x^2/2} \tag{3}$$

Sigmoid function serves as excitation function in output layer and the formula is given in (4):

$$\sigma(u) = 1\big/(1+e^{-u}) \tag{4}$$

Training sample set as $X=[X_1, X_2, \cdots, X_M]$, in which *M* is the number of samples, and corresponding actual output is $Y=[Y_1, Y_2, \cdots, Y_N]$, the element of which can be calculated via (5). And, the expected output is $\hat{Y} = [\hat{Y}_1, \hat{Y}_2, ..., \hat{Y}_N]$. *N* is the number of outputs. The samples number is equal to the number of input layers. Similarly, the number of outputs is equal to the number of output layers in WNN.

And summation of output layer energy error is $E(N)$. Its equation is given in (6):

$$Y_i = \sigma(u_i) = \sigma\left[\sum_{k=1}^{K} \omega_{kn} \psi_{a_k, b_k}\left(\sum_{m=1}^{M} \omega_{mk} x_m\right)\right] \tag{5}$$

$$E(N) = 1\big/(2N) \sum_{i=1}^{N} (\hat{Y}_i - Y_i)^2 \tag{6}$$

Each node determined, it is critical to choose appropriate parameters (ω_{mk}, a_k, b_k, ω_{kn}) for constructing neural networks. The weight between the *m*-th input layer and the *k*-th hidden layer is ω_{mk}. Meanwhile the weight between the *k*-th hidden layer and the *n*-th output layer is ω_{kn}. Moreover the scale factor and the displacement factor in the *k*-th hidden layer are a_k and b_k respectively in the WNN. The algorithm APSO is adopted to search the optimal parameters in the WNN.

ADAPTIVE PARTICLE SWARM OPTIMIZATION WAVELET NEURAL NETWORK (APSO-WNN)

PSO algorithm is proposed by Kennedy in 1951. And it was inspired by natural biological clusters. The basic idea is that each particle in the algorithm has the ability of self-recognition and of social learning (Zhihuai, 2015) (Ramezanpour, 2018). So that the particle swarm is eventually assembled into an optimal particle to obtain the optimal solution. The proposed APSO is based on traditional PSO. The different inertia weights are adopted in the different particles in order to achieve the adaptive weight in the process of iterating. In s-dimensional space, $X_i=(x_{i1}, x_{i2}, \cdots, x_{is})$ is the particle position vector of the *i*-th particle, and $V_i=(v_{i1}, v_{i2}, \cdots, v_{is})$ is the corresponding particle velocity vector. $P_i=(p_{i1}, p_{i2}, \cdots, p_{is})$ is its optimal position, while $P_g=(p_{g1}, p_{g2}, \cdots, p_{gs})$ is the optimal position of the whole swarm. During iterating, the speed and the position of each particle are updated according to (7) and (8) respectively.

$$V_i(j+1) = wV_i(j) + c_1 r_1 [P_i - x_i(j)] + c_2 r_2 [P_g - X_i(j)] \tag{7}$$

$$X_i(j+1) = X_i(j) + V_i(j+1) \tag{8}$$

Where j is the number of iterations and w is the inertia weight. The accelerating factor and social factors are c_1 and c_2 respectively, usually equal to 2. The random numbers between 1 and 0 are r_1 and r_2. It is known that the inertia weight w plays a critical role in the process of searching. The scheme of APSO-WNN is listed as follows.

① Initialize particle swarm; The particle dimension is selected and the particle position is determine according to the WNN parameters (ω_{mk}, a_k, b_k, ω_{kn}). The value of inertia weight w_0, accelerating factor and maximum iterating number are initialized in this step. The precedent iteration number is equal to 1.

② The accuracy error of the network is used as the goal function to calculate the fitness.

③ The fitness of precedent particle is compared with the corresponding individual extremum. Update the individual extreme fitness with the lesser one and the corresponding particle position to be local extremum.

④ The minimum fitness of all particles is employed as the group extreme fitness, and the corresponding position is used as the group extremum.

⑤ Adaptive adjustment of the weights: The fitness of P_i is f_i, and the corresponding optimal particle fitness is $f_{\min}$. The average fitness of particles is $\overline{f}$.

When the particle fitness is less than $\overline{f}$, the particle is close to the global optimum. At this point, a smaller inertia weight should be used to stabilize the global optimum, and the equation is shown as Eq. (9).

$$w = w_0 \times \frac{f_i - f_{\min}}{\overline{f} - f_{\min}} \tag{9}$$

When the particle fitness is greater than $\overline{f}$, which is worse than all particles. A larger inertia weight should be applied to reach the global optimum faster. The equation is shown in Eq. (10).

$$w = 1.5 - \frac{1}{1 + \exp[q(f_i - \overline{f})]} \tag{10}$$

Where q is a constant more than 0, and w_0 is an appropriate value between 0 and 1.

⑥ The positions of every particle are changed according to (8). Set position $X_i \in [X_{min}, X_{max}]$. Let X_i equal to X_{min}, when $X_i < X_{min}$. On the contrary, let X_i equal to X_{max}.

⑦ The PSO algorithm is finished when the number of iterations reaches the maximum, or the fitness is satisfied. Otherwise turn to ②.

NUMERICAL EXPERIMENT

In order to evaluate the performance of APSO algorithm, unimodal functions (Yong, 2011) and multimodal functions (Yong, 2011) used to verify the local search ability, global search ability and convergence performance of the proposed algorithm. The two-dimensional graphs of four test functions corresponding to F1-F4 in Appendix Ⅰ are shown in Figure 2, respectively. The $u(\cdot)$ in multimodal functions (Yong, 2011) F3 and F4 is shown in Appendix Ⅰ.

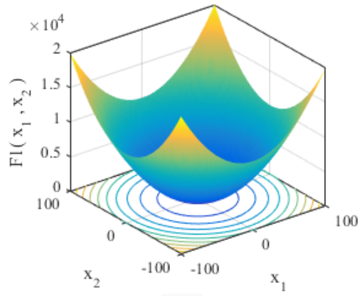

(a) F1 function.

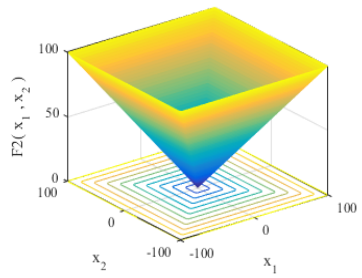

(b) F2 function.

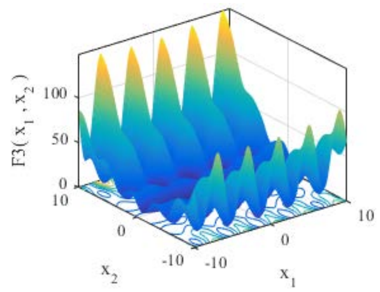

(c) F3 function.

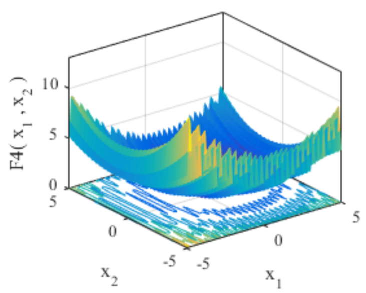

(d) F4 function.

Fig. 2. The benchmark mathematical functions.

Table 1. The numerical results of benchmark mathematical functions.

Function	Metric	PSO	FA	GA	FOA	APSO
F1	Mean	0.000134	1.9322e-26	3.1571e-7	4.3764e-8	0.2231e-33
	Std	0.000201	0.7843e-23	2.3624e-6	3.2236e-8	0.3187e-30
F2	Mean	0.006498	2.1053e-13	1.3387e-4	1.3187e-8	5.11e-25
	Std	0.026226	5.3542e-12	1.4372e-3	1.5769e-7	1.45e-21
F3	Mean	0.009178	6.3136e-15	1.7826e-3	1.82e-5	0.3733e-15
	Std	0.007613	2.4725e-14	1.9835e-3	2.23e-4	0.2831e-13
F4	Mean	1.086375	2.4616e-11	0.15723	0.65472	0.5172e-11
	Std	0.315027	1.5232e-10	0.06361	1.45913	0.2497e-9

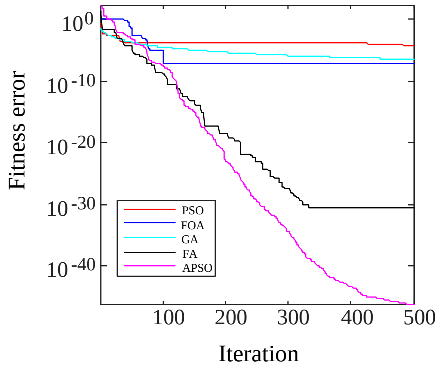

(a) The iterative curve of the algorithms in F1.

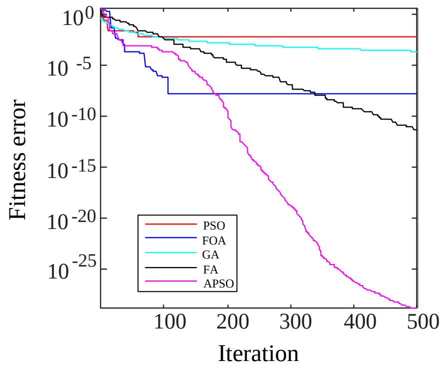

(b) The iterative curve of the algorithms in F2.

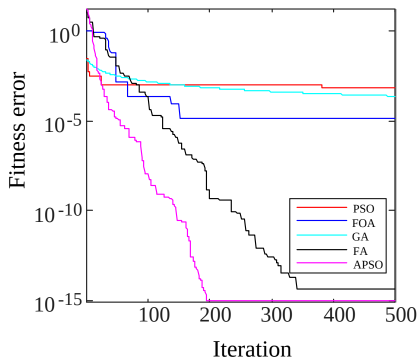

(c) The iterative curve of the algorithms in F3.

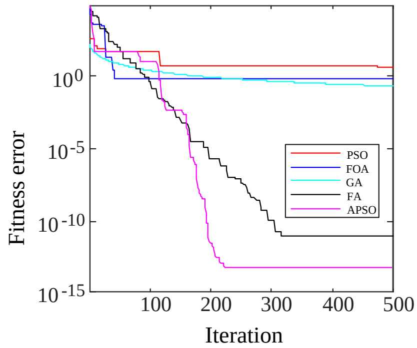

(d) The iterative curve of the algorithms in F4.

Fig. 3. The convergence curves of five algorithms in four benchmark mathematical functions.

The subfigures (a)、(b)、(c) and (d) in Figure 3 are the convergence curves of five algorithms in four benchmark mathematical functions respectively. According to Fig. 3, APSO algorithm is superior to other algorithms in F1 and F2 while FOA algorithm is superior to APSO in F3, but its iteration times are greater than that in the APSO algorithm. The traditional PSO algorithm has the worst ability to deal with the F4. The APSO algorithm is better than FA algorithm in the F4, but its iteration times are greater than FA algorithm. In summary, APSO has better comprehensive optimization ability than other algorithms.

Table 2. The coefficients setting of optimization algorithms.

Optimization algorithm	Algorithm parameters
FOA	Population size: 20
	Maximum number of iteration: 500
FA	Attractiveness coefficient: 1.0
	Light absorption coefficient: 0.8
GA	Crossover probability: 0.7
	Mutation probability: 0.01
PSO	Learning factor 1: 1.5
	Learning factor 2: 1.5
APSO	Study factor 1: 2
	Study factor 2: 2

The paper compares APSO with traditional PSO algorithm (Li, 2018), fruit fly optimization algorithm (FOA) (Guo, 2018), genetic algorithm (GA) (Koopialipoor, 2019) and firefly algorithm (FA) (Danandeh, 2018). The overall size of the algorithm is 30, the optimization dimension D is 20, and each algorithm is tested 30 times independently. And the mean and standard deviation (Std) of the error value of each algorithm function are calculated. The results are shown as Table 1. The parameters of five algorithms are shown in Table 2.

From Appendix Ⅰ and Table 1 it can be seen that local optimization ability in the APSO algorithm on unimodal function is stronger than that in the FA algorithm, and the optimization of two multimodal functions shows that the two algorithms have their own advantages. As an improvement of the traditional PSO algorithm, APSO performs better than the traditional PSO algorithm.

FAULT DIAGNOSIS OF HYDRO-GENERATION

Fault Analysis of Hydroelectric Generating Set

The relationship between fault types and vibration characteristics is nonlinear extremely because of the nonlinear system in hydro-generation. The vibrations in the HGU are so complicated that the vibrations can be divided into the hydraulic vibration, the mechanical vibration and the electromagnetic vibration (Ma, 2017). These three kinds of vibration often exist and interact with each other. At present, the vibration signal of HGU is needed to realize fault diagnosis.

Failure Characteristics and Simulation Parameters Selection

A large number of fault information is included in the HGU vibration signal, so vibration signal often serves as a kind of characteristic to diagnose the fault. In this paper, the energy of HGU vibration signal is applied as the input signal of the neural network. According to (Hidalgo, 2014), the time-domain waveform and the frequency-domain waveform of three kinds of fault signals are shown in Fig. 3 and Figure 4 respectively.

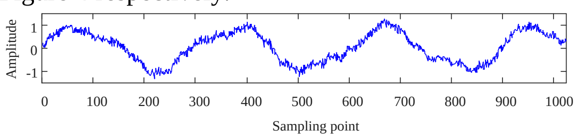

(a) The waveform of vortex band eccentricity failure

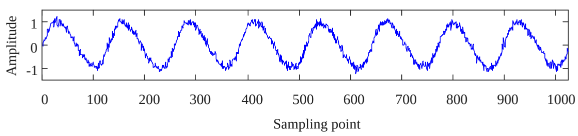

(b) The waveform of unbalance failure

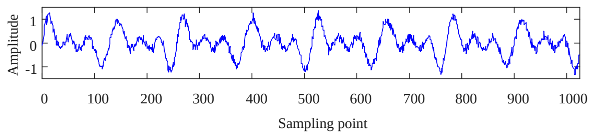

(c) The waveform of shafting system misalignment failure

Fig. 4. The time-domain waveform.

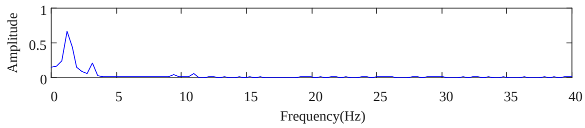

(a) The spectrum of vortex band eccentricity failure

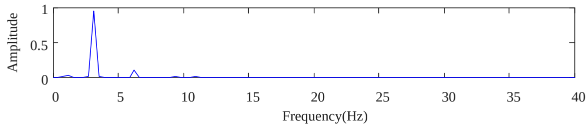

(b) The spectrum of unbalance failure

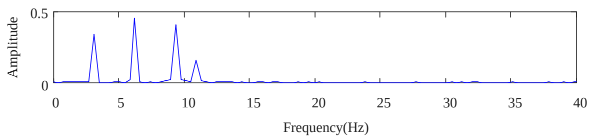

(c) The spectrum of shafting system misalignment failure

Fig. 5. The frequency-domain waveform.

Some researches have been conducted for the vibration fault of HGU (Wenji, 2007)(Zhang, 2019). The spectral characteristics of the vibration signal in HGU obtained from the experiments are taken as the fault features, including the amplitude components of the five feature bands (0.4-0.5)f, 1f, 2f, 3f and >3f. Here f is the units running frequency.

The Vortex band eccentricity is shown in the Fig. 4 (a). The unbalance of the HGU is shown in the Fig. 4 (b). The hydroelectric generating units shafting system misalignment is shown in the Fig. 4 (c). The subfigures (a)、(b) and (c) in Figure 5 are the spectrum of the subfigures (a)、(b) and (c) in Fig. 4 respectively.

1. The main feature of Vortex band eccentricity is that the vortex band rotates in the draft tube, resulting in the low-frequency pressure pulsations of the water flow and the vibrations of related devices. And the corresponding characteristic signal is mainly reflected at 0.4-times to 0.5-times for the rotation frequency.

2. The Unbalance of the HGU is caused by the rotor quality imbalance. It contains the following characteristics: its amplitude is proportional to the

square of the rotation frequency; and the main frequency of the vibration signal is the rotation frequency.

3. The shafting vibration of the unit is obvious, when the unit is running at no-load or low-speed conditions. This is the main features of the HGU shafting system misalignment. And the fault characteristic signal is mainly reflected from the double rotation frequency and triple rotation frequency. Notion that the double frequency component characteristics are significant especially.

The simulations were conducted by the algorithm APSO-WNN to diagnose the fault of HGU. The input node number is set to 5, and the output layer is set to 4. The hidden layer node is set to 9 according to experience. The maximum number of iterations is selected to be 100 in APSO. The particle number is set to 20. The initial value of inertia weight is set to 0.4. The tolerance of the neural network output is selected to be 0.001.

In this paper, the amplitude components of five characteristic bands are used as APSO-WNN fault data sets. The distribution of these amplitude components in each frequency band is shown in Figure 6. It can be seen that the amplitude components of "Vortex band eccentricity" and "Unbalance" faults are larger in low frequency band, and their fault characteristics are obvious. However, the amplitude components of "Misalignment" fault distribute uniformly in the whole frequency band, and its fault characteristics are not obvious. While HGU does not fail (Normal), the magnitude component of the "fault" in each frequency band is small.

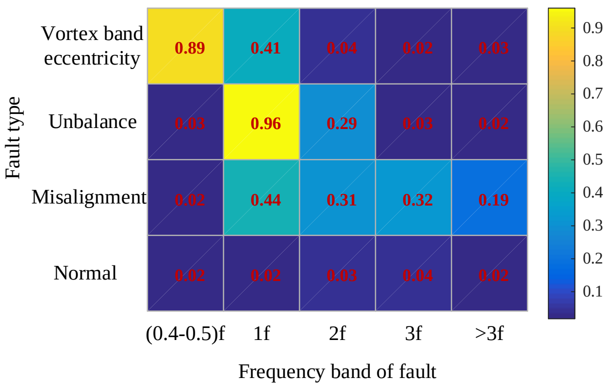

Fig. 6. The characteristics distribution map of 4 faults.

Table 3. The training samples.

Fault types	(0.4-0.5)f	1f	2f	3f	>3f	Target output
A	0.88	0.22	0.02	0.04	0.06	0 0 0 1
	0.90	0.20	0.05	0.02	0.02	0 0 0 1
	0.92	0.21	0.03	0.01	0.04	0 0 0 1
	0.85	0.23	0.06	0.03	0.01	0 0 0 1
	0.91	0.21	0.03	0.01	0.01	0 0 0 1
	0.86	0.23	0.06	0.03	0.02	0 0 0 1
	0.87	0.22	0.05	0.04	0.04	0 0 0 1
	0.93	0.20	0.02	0.02	0.06	0 0 0 1
	0.89	0.23	0.01	0.01	0.03	0 0 0 1
	0.93	0.23	0.04	0.03	0.02	0 0 0 1
B	0.04	0.98	0.10	0.02	0.02	0 0 1 0
	0.02	1.00	0.08	0.03	0.01	0 0 1 0
	0.05	0.90	0.11	0.05	0.02	0 0 1 0
	0.03	0.96	0.12	0.04	0.03	0 0 1 0
	0.05	0.90	0.11	0.05	0.01	0 0 1 0
	0.03	0.98	0.08	0.02	0.02	0 0 1 0
	0.04	1.00	0.12	0.03	0.03	0 0 1 0
	0.04	0.96	0.10	0.04	0.03	0 0 1 0
	0.01	0.97	0.09	0.01	0.01	0 0 1 0
	0.02	0.95	0.13	0.02	0.02	0 0 1 0
C	0.02	0.41	0.43	0.34	0.15	0 1 0 0
	0.01	0.52	0.40	0.32	0.10	0 1 0 0
	0.01	0.40	0.47	0.35	0.18	0 1 0 0
	0.03	0.45	0.42	0.28	0.29	0 1 0 0
	0.01	0.52	0.47	0.35	0.18	0 1 0 0
	0.03	0.40	0.40	0.32	0.10	0 1 0 0
	0.01	0.41	0.42	0.28	0.29	0 1 0 0
	0.02	0.45	0.43	0.34	0.15	0 1 0 0
	0.01	0.44	0.44	0.33	0.28	0 1 0 0
	0.03	0.43	0.45	0.29	0.16	0 1 0 0
D	0.01	0.02	0.01	0.05	0.04	1 0 0 0
	0.01	0.03	0.02	0.03	0.02	1 0 0 0
	0.02	0.01	0.05	0.07	0.01	1 0 0 0
	0.02	0.04	0.06	0.01	0.03	1 0 0 0
	0.03	0.01	0.02	0.07	0.02	1 0 0 0
	0.01	0.03	0.06	0.05	0.03	1 0 0 0
	0.01	0.04	0.01	0.03	0.01	1 0 0 0
	0.02	0.02	0.05	0.01	0.04	1 0 0 0
	0.02	0.01	0.04	0.02	0.01	1 0 0 0
	0.03	0.02	0.03	0.04	0.02	1 0 0 0

A: Vortex band eccentricity; B: Unbalance; C: Misalignment; D: Normal

Table 4. The part of the test samples.

Fault types	A	B	C	D
(0.4-0.5)f	0.82	0.02	0.01	0.01
1f	0.28	0.91	0.48	0.05
2f	0.05	0.08	0.48	0.02
3f	0.04	0.01	0.36	0.03
>3f	0.03	0.02	0.20	0.01
Target output	0 0 0 1	0 0 1 0	0 1 0 0	1 0 0 0

A: Vortex band eccentricity; B: Unbalance; C: Misalignment;
D: Normal

The part of training samples is shown in the Table 3 and the part of testing samples is shown in the Table 4. Four elements in the target-output represent 4 types of faults respectively, in which the number 1 represents failure and the number 0 is non-failure in Table 3 and Table 4.

Result and Analysis of Vibration Fault Diagnosis for Hydroelectric Generating Units

In order to prove the validity of the APSO-WNN and its advantages, the same neural network parameters are employed on the same computer. APSO-WNN, momentum gradient BP neural network (Na, 2014) and WNN are all trained by learning samples. Then input the test samples to networks.

Table 5. The Test result of three algorithms.

Fault types	Methods
	BP neural network
A	0.27,-0.13,0.27, 0.77
B	0.26,0.18,0.83,0.12
C	0.36,0.72,0.34,0.15
D	0.67, -0.01,-0.01,0.01
	WNN
A	0.09,-0.04,0.15,0.95
B	0.13,0.08,0.88,0.18
C	0.25,0.91,0.13,-0.07
D	0.92,-0.13,0.08,0.07
	APSO-WNN
A	-0.03,-0.01,0.02,1.02
B	0.02,-0.04,0.99,0.11
C	-0.24,0.97,0.04,-0.01
D	1.00,-0.01,-0.01,0.02

A: Vortex band eccentricity; B: Unbalance; C: Misalignment;
D: Normal.

The 4 faults output corresponding to the different algorithms are shown in Table 5. The closer to 1 the value is, the higher the probability of failure is. Otherwise the lower the probability of failure is. The training curves are shown in Figure 7, Figure 8, Figure 9 and Figure 10.

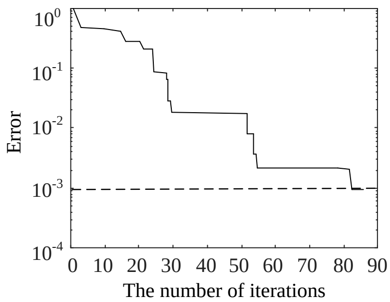

Fig. 7. The training curve of APSO-WNN.

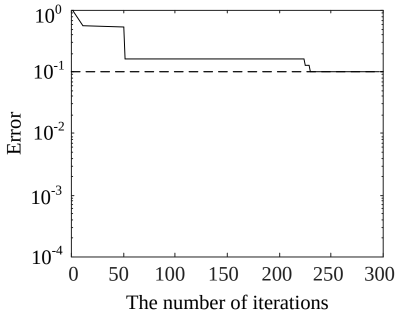

Fig. 8. The training curve of BP neural network.

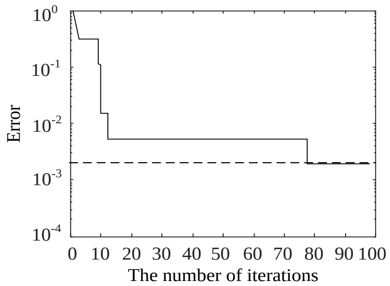

Fig. 9. The training curve of WNN.

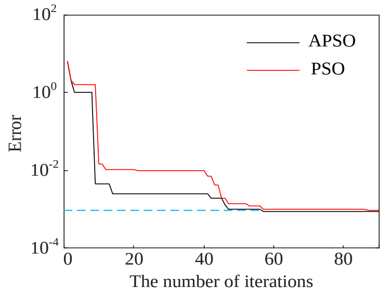

Fig. 10. The training curves of APSO and PSO.

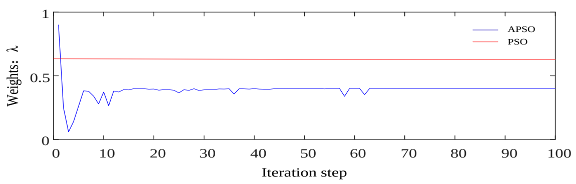

Fig. 11. The weight curves of the APSO and the PSO.

From the results of Fig. 7, Fig. 8 and Fig. 9, it can be observed that the error trained by learning samples via momentum gradient BP neural network can reach to 0.1 after 300 iterations. And error trained by the same samples via APSO-WNN can reach to 0.001 after 83 iterations. While the ones trained via the wavelet neural network can also be within 0.01 after 100 iterations. It can be observed in Table 5 that the results versus BP neural network can be used to diagnose the vibration fault types of hydraulic turbine generator units at a certain degree. But results versus APSO-WNN are significantly closer to target output, compared with the performance of the results of wavelet neural network. Meanwhile, weight curves of APSO and PSO are shown in Fig. 10. By comparing APSO and PSO, it can be found that during the 83-th iteration, APSO shows less error than PSO, which means the APSO can obtain a more suitable weight, while the weight of PSO is fixed. In order to change the training error, the initial weight of PSO must be changed at each iteration incessant.

In this paper, 160 sets of fault samples are used to further verify the diagnostic ability of the proposed method for four kinds of faults. The first 80 fault data sets are used as training samples, and 20 training samples are used for each fault. The second 80 fault data sets are used as test samples, with 20 test samples for each fault. Then the four kinds of fault diagnosis algorithms (FOA-WNN(Jing, 2016)、PSO-WNN(Deyun, 2018), GA-WNN(Jiahong, 2015), FA-WNN(Senapati, 2013) are compared, and the diagnosis results of each algorithm are shown in Table 6.

It can be seen in Fig. 6 that the fault signals generated by the HGU are distributed at a low level in five frequency bands while the HGU is in the "normal" state (no fault occurs). Therefore, the recognition rate of five algorithms for normal "fault" is higher and they are equal to 95% shown in Table 6.

Table 6. The diagnostic results of different algorithm.

Fault type	Number of test samples	Correct number diagnoses				
		A	**B**	**C**	**D**	**E**
Vortex band eccentricity	20	17	18	17	16	18
Unbalance	20	18	17	16	15	18
Misalignment	20	14	12	15	11	17
Normal	20	19	19	19	19	19

A: FOA-WNN; B: FA-WNN; C: GA-BP; D: PSO-BP; E: APSO-WNN

Vortex band eccentricity and Unbalance have the obvious characteristics in distribution of frequency band. The proposed algorithm is identical with FA-WNN in identifying Vortex band eccentricity faults and the correct recognition rate can achieve 90%. Similarly, FOA-WNN and the proposed algorithm are identical in identifying Unbalance faults and the correct recognition rate can reach 90%.

"Misalignment" is one of the most difficult identified faults because its characteristics in each frequency band are not obvious enough. Therefore, the recognition rate of each algorithm for Misalignment is low, but the recognition rate in the proposed algorithm is higher, up to 85%. In summary, the proposed algorithm has a strong ability to identify faults comprehensively.

CONCLUSIONS

The proposed APSO-WNN algorithm can better combine APSO algorithm with WNN algorithm, and has stronger recognition ability for four fault types.

1) APSO algorithm improves the global search ability and convergence performance of PSO algorithm. For unimodal functions, the optimal solution accuracy of the proposed algorithm can reach 0.2231e-33. For multimode functions, the optimal solution accuracy of the proposed algorithm is up to 0.3733e-15.

2) APSO-WNN has lower diagnostic error. Compared with the traditional BP neural network and WNN algorithm, after 83 iterations, the error can reach 0.01.

3) APSO-WNN has a good diagnostic rate for fault types. Compared with FOA-WNN, FA-WNN, GA-BP and PSO-BP, the proposed algorithm can diagnose the four faults of "Vortex band eccentricity", "Unbalance", "Misalignment" and "Normal" with a correct rate of 90%, 90%, 85% and 95% respectively.

ACKNOWLEDGMENT

This work was supported in part by a grant from the scientific research foundation for the returned overseas Chinese scholars, state education ministry (grant number KJ2015QT007)

REFERENCES

Jianwei L, Liangyu X, Chao T, Yongheng L, “Cause Analysis of Low Frequency Vibration of Flexible Support Stator Frame for Giant Hydro Generator,” *J. Vib. Conntrol*, Vol. 22, No. 14, pp. 3151-3156 (2016).

Mahdi K, Jianhui W, “Spatio-Temporal Graph Deep Neural Network for Short-term Wind Speed Forecasting,” *IEEE T. Sustain. Energ.*, Vol. 10, No. 2, pp. 670-681 (2019).

Jia W, Zhao D, Zheng Y, et al, “A Novel Optimized GA-Elman Neural Network Algorithm,” *Neural Comput. Appl.*, Vol. 10, No.2, pp. 670-681 (2019).

Xiaochuan S, Guan G, Yingqi L, et al, “ResInNet: A Novel Deep Neural Network with Feature Re-use for Internet of Things,” *IEEE Internet Things* Vol. 6, No. 1, pp. 679-691 (2018).

Ma L, Wang B, Yan S, et al, “Temperature Error Correction Based on BP Neural Network in

Meteorological Wireless Sensor Network," *INT. J. Sens. Netw.*, Vol. 23, No. 4, pp. 265-278 (2017).

Zhang B D, Tian Y, Zhou J P, et al, "Vibration Fault Diagnosis of a Hydro-Generating Unit Based on Choquet Fuzzy Integration," *Shock Vib.*, Vol. 32, No. 12, pp. 61-66 (2013).

Jiatang C, Zhimei D, Yan X, "QAPSO-BP Algorithm and its Application in Vibration Fault Diagnosis for a Hydroelectric Generating Unit," *Shock Vib.*, Vol. 34, No. 23, pp. 177-182 (2015).

M.H.R Fard, M Basri, A Kassim, et al, "Optimization of Process Parameters for Lipase-Catalyzed Synthesis of Steramines-Based Esterquats Using Wavelet Neural Network (WNN) in 2-Liter Bioreactor," *J. Ind. Eng. Chem.*, Vol. 20, No. 4, pp. 1973-1976 (2014).

Lifeng W, Beibei Y, Zhen P, et al, "Fault Diagnosis of Roller Bearings Based on, a Wavelet Neural Network and Manifold Learning," *Appli. Sci.*, Vol. 7, No. 2, pp. 158-171 (2017).

Yanchun X, Yufei D, Shan C, et al, "A Method of De-Noise and Harmonics Detection in Power System Based on Periodicity Analysis," *Mapan-J. Metrol. Soc. I.*, Vol. 33, No. 2, pp. 1-9 (2018).

Zhenhua L, Yuan T, Abu-Siada A, et al, "A New Vibration Testing Platform for Electronic Current Transformers," *IEEE T. Instrum. Meas.*, Vol. 68, No. 3, pp. 704-712 (2019).

Amezquita-Sanchez J P, Adeli H, "Signal Processing Techniques for Vibration-Based Health Monitoring of Smart Structures," *Arch. Comput. Method. E.* Vol. 23, No. 1, pp.1-15 (2016).

Cha Y J, Buyukozturk O, "Structural Damage Detection Using Modal Strain Energy and Hybrid Multiobjective Optimization," *Comput-Aided. Civ. Inf.*, Vol. 30, No. 5, pp. 347-358 (2015).

Zhihuai X, Zhaohui S, Libo S, et al, "Simulated Annealing-Wavelet Neural Network for Vibration Fault Diagnosis of Hydro-Turbine Generating Unit," *J. Optoelectron. Adv. M.*, Vol. 17, No.56, pp. 734-740 (2015).

Ramezanpour M, Siavashi M., "Application of SiO2-Water Nano fluid to Enhance Oil Recovery," *J. Therm. Anal. Calorim.*, Vol. 135, No. 1, pp. 565-580 (2018).

Yong L, Kwong-Sak. L, "Genetic Algorithm with Adaptive Elitist-Population Strategies for Multimodal Function Optimization," *Appl. Soft Comput.*, Vol. 11, No. 2, pp. 2017-2034, (2011).

Li H, Yang D, Su W, et al, "An Overall Distribution Particle Swarm Optimization MPPT Algorithm for Photovoltaic System under Partial Shading," *IEEE T. Ind Electron.*, Vol. 66, No. 1, pp. 265-275 (2018).

Guo Q, Quan Y, Jiang C, "Object Pose Estimation in Accommodation Space Using an Improved Fruit Fly Optimization Algorithm," *J. Intell. Robot Syst.*, Vol. 95, No. 2, pp. 405-417 (2018).

Koopialipoor M, Armaghani D.J., Haghighi M, et al, "A Neuro-Genetic Predictive Model to Approximate over Break Induced by Drilling and Blasting Operation in Tunnels," *B. Eng. Geol. Environ.*, Vol. 78, No. 2, pp. 981-990 (2019).

Danandeh Mehr A, Nourani V, Karimi Khosrowshahi V, et al, "A Hybrid Support Vector Regression-Firefly Model for Monthly Rainfall Forecasting," *Int. J. Environ. Sci. Te.*, Vol. 16, No. 1, pp. 335-346 (2018).

Hidalgo L.G., Fontane D.G., Lopes J.E.G, "Efficiency Curves for Hydroelectric Generating Units," *J. Water. Res. Plan. Man.*, Vol. 140, No. 1, pp. 86-91 (2014).

Wenji P, Xingqi L, Pengcheng G, "Vibration Signal Preprocessing of Hydraulic Generator set Based on the Second Generation Wavelet," *Proceedings of the CSEE*, Vol. 27, No. 30, pp. 103-107, (2007).

Zhang J, Wen H, Tang L, "Improved Smoothing Frequency Shifting and Filtering Algorithm for Harmonic Analysis with Systematic Error Compensation," *IEEE T. Ind. Electron.*, Vol. 66, No. 12, pp. 9500-9509 (2019).

Na L, Zhi-huai X, Xiangian F, "Vibration Fault Diagnosis of Hydroelectric; Generating Unit Based on ACO-Initialized Wavelet Network," *J. Hydro. Eng.*, Vol. 33, No. 2, pp. 251-258 (2014).

Jing X, Zhongbin W, Chao T, et al, "Adaptive Wavelet Threshold De-Noising Method for Machinery Sound Based on Improved Fruit Fly Optimization Algorithm," *Appli. Sci.*, Vol. 6, No. 7, pp. 199-214 (2016).

Deyun W, Yan l, Zeng W, et al, "Scenario Analysis of Natural Gas Consumption in China Based on Wavelet Neural Network Optimized by Particle Swarm Optimization Algorithm," *Energies*, Vol. 11, No. 4, pp. 825-841 (2018).

Jiahong Z, Yusheng W, Qingquan L, et al, "Research on High-Precision, Low Cost Piezo resistive, MEMS-Array Pressure Transmitters Based on Genetic Wavelet Neural Networks for Meteorological Measurements," *Micromachines*, Vol. 6, No.5, pp. 554-573 (2015).

Senapati M.R., Dash P.K., "Local Linear Wavelet Neural Network Based Breast Tumor Classification Using Firefly Algorithm," *Neural Comput. Appl.*, Vol. 22, No. 7, pp. 1591-1598 (2013).

APPENDIX

I. The formula of F1～F4 function are as follows.

$$\mathrm{F1}(x)=\sum_{i=1}^{D}x_i^2 \tag{11}$$

$$\mathrm{F2}(x)=\max_i\left\{\left|x_i\right|,1\le i\le D\right\} \tag{12}$$

$$\mathrm{F3}(x)=\frac{\pi}{n}\left\{\begin{matrix}10\sin(\pi y_1)\\ +\sum_{i=1}^{n-1}(y_i-1)^2\left[1+10\sin^2(\pi y_{i+1})\right]\\ +(y_n-1)^2\end{matrix}\right\}$$

$$+\sum_{i=1}^{n}u(x_i,10,100,4) \tag{13}$$

$$y_i=1+\frac{x_i+1}{4}u(x_i,10,100,4)$$

$$\mathrm{F4}(x)=0.1\left\{\begin{matrix}\sum_{i=1}^{n}(x-1)^2[1+\sin^2(3\pi x_i+1)]\\ +(x_n-1)^2[1+\sin^2(2\pi x_n)]\\ +\sin^2(3\pi x_1)\end{matrix}\right\} \tag{14}$$

$$+\sum_{i=1}^{n}u(x_i,5,100,4)$$

$$u(x_i,a,k,m)=\begin{cases}k(x_i-a)^m & x_i>a\\ 0 & -a<x_i<a\\ k(-x_i-a)^m & x_i<-a\end{cases} \tag{15}$$

NOMENCLATURE

ω_{mk} the weight between the m-th input layer and the k-th hidden layer in wavelet neural network

ω_{kn} the weight between the k-th input layer and the n-th hidden layer in wavelet neural network

$\sigma(u)$ the sigmoid function in wavelet neural network

$E(n)$ the summation of output layer energy error in wavelet neural network

$\psi_{(x)}$ the wavelet functions

w the inertia weight in APSO

X_i the particle position vector of the i-th particle in APSO

V_i the corresponding particle velocity vector in APSO

P_i optimal position in APSO

P_g optimal position of the whole swarm in APSO

f_i the fitness in APSO

c_1 the accelerating factor in APSO

c_2 the social factor in APSO

APSO-WNN 及其在水電機組振動故障診斷中的應用研究

徐艷春　夏海廷　方紹晨
三峽大學梯級水電站運行與
控制湖北省重點實驗室

呂密
德克薩斯農工大學電氣與計算機工程學院

摘 要

在小波神經網絡研究的基礎上，針對水電系統震動特性與故障類型之間複雜的非線性關係，提出了一種自適應粒子群優化算法。該算法結合了進化計算和群體智能的特點。它可以根據粒子的狀態自適應地改變慣性權重。自適應粒子群優化算法提高了小波神經網絡的訓練速度，提高了網絡的訓練精度。實驗表明，與 BP 神經網絡、小波神經網絡相比，基於自適應粒子群優化算法的小波神經網絡具有更高的診斷精度和更快的診斷速度。該算法是水電機組故障診斷的一種新方法，可有效應用於實際工程中。